Intracellular Calcium Waves Accompany Neutrophil Polarization, Formylmethionylleucylphenylalanine Stimulation, and Phagocytosis: A High Speed Microscopy Study[1]

Andrei L. Kindzelskii and Howard R. Petty[2]

Using high sensitivity fluorescence imaging with shutter speeds ~600,000 times faster than those of video frames, we have characterized Ca^{2+} waves within cells in exquisite detail to reveal Ca^{2+} signaling routes. Polarized neutrophils exhibited a counterclockwise rotating ryanodine-sensitive juxtamembrane Ca^{2+} wave during temporal calcium spikes. During stimulation with fMLP, a chemotactic factor, two Ca^{2+} waves traveling in opposite directions around the perimeter of the cell emanated from sites of stimulation (the clockwise wave is verapamil sensitive). Phagocytosed targets exhibit counterclockwise Ca^{2+} waves traveling about their periphery originating from the plasma membrane. This study: 1) outlines the technology to observe Ca^{2+} signaling circuitry within small living cells; 2) shows that extracellular spatial information in the form of a chemotactic factor gradient is transduced into intracellular chemical patterns, which provides fresh insights in signaling; 3) suggests that a line of communication exits between the cell surface and phagosomes; and 4) suggests that spatiotemporal Ca^{2+} patterns contribute to drug actions. ***The Journal of Immunology,*** **2003, 170: 64–72.**

Transmembrane signaling is conventionally viewed as the appearance of a second messenger such as Ca^{2+}, cAMP, or phosphoproteins within the cytoplasm of a cell (1). However, recent studies have shown that signaling can be mediated by temporal changes in second messenger concentrations. For example, intracellular Ca^{2+} concentration changes can lead to differential gene expression (2). Intracellular Ca^{2+} levels oscillate as well, with frequency-encoded information (3–8). In addition to temporal Ca^{2+} changes, its concentration may also vary spatially within a cell. Many studies have reported static Ca^{2+} gradients (9, 10), which presumably reflect Ca^{2+} source and sink terms some distance apart. However, such images contain little temporal information. Experiments to derive spatiotemporal information generally represent long time-scale variations in "static" patterns, not inherent dynamics. Examples of slowly changing Ca^{2+} patterns include hepatocytes, endothelial cells, neutrophils, and exocrine cells (11–15). Spatiotemporal Ca^{2+} waves have been observed in large cells including oocytes and myocytes and in cell layers (16–19). However, it has been impossible to observe such waves in small cells due to rapid wave motion, intermixing of cytoplasmic labels during image acquisition, and comparatively high background levels at typical exposure times.

To study spatiotemporal Ca^{2+} waves in small cells, such as neutrophils, mast cells, and lymphocytes, a technique with high spatial and temporal resolution is required. High resolution perpendicular to the optical axis a microscope (lateral or *x-y*) is provided by conventional microscopy, which provides a resolution of ~200 nm according to Rayleigh's equation. The temporal resolution required depends on the dynamics of the events under study. Assuming that a wave travels at an unmyelinated axon velocity (~10 m/s), a 50-ns exposure time leads to an acceptable wave displacement of 500 nm while the shutter is open. Some blurring is anticipated, but the displacement is a fraction of the cell size. Previous studies in other cell types have reported Ca^{2+} wave velocities of ~25 μm/s (16–18). In this case, a 1-ms exposure yields a displacement of 25 nm, which is much smaller than the Rayleigh distance. Thus, depending on the underlying mechanism(s), biological wave phenomena may require shutter speeds of 50 ns to 1 ms.

Several high speed microscopy techniques have been developed to explore this time regimen. To shorten exposure times, Zoghbi et al. (20) excited intracellular fluorescence using a single-shot 7-ns laser pulse. Although these short pulses eliminated blurring during exposure, one could not collect a consecutive image series of Ca^{2+} signals. Recent developments in high speed imaging have relied primarily on charge-coupled device (CCD)[3] technology. This approach has yielded capture rates of ~100 to 1000 frames/s (19–22) wherein the exposure time was equal to the frame readout time. We have recently developed a high speed microscopic imaging technique that captures individual images with 50 ns to ms exposure times at up to 1000 frames/s (23–26), which allows us to collect stop-action movies of extremely rapid cell signaling events.

In the present study, we extend our high speed microscopy studies to intracellular Ca^{2+} signaling. Our work suggests novel elements of Ca^{2+} signaling processes in human neutrophils including Ca^{2+} pattern reorientation during chemotactic stimulation and plasma membrane-to-phagosome signaling after phagocytosis.

Materials and Methods

Materials

Reagents were obtained from Sigma-Aldrich (St. Louis, MO) unless otherwise noted. Indo-1-acetoxymethyl ester (indo-1-AM) and BAPTA-AM were purchased from Molecular Probes (Eugene, OR).

Department of Biological Sciences, Wayne State University, Detroit, MI 48202

Received for publication June 24, 2002. Accepted for publication October 23, 2002.

The costs of publication of this article were defrayed in part by the payment of page charges. This article must therefore be hereby marked *advertisement* in accordance with 18 U.S.C. Section 1734 solely to indicate this fact.

[1] This work was supported by National Institutes of Health Grant CA74120 (to H.R.P.).

[2] Address correspondence and reprint requests to Dr. Howard R. Petty, Department of Biological Sciences, Wayne State University, Detroit, MI 48202. E-mail address: hpetty@biology.biosci.wayne.edu

[3] Abbreviations used in this paper: CCD, charge-coupled device; indo-1-AM, indo-1-acetoxymethyl ester; ER, endoplasmic reticulum.

0022-1767/03/$02.00

Cells

Human peripheral blood neutrophils were purified using Ficoll-Hypaque step density gradient centrifugation. The cells were labeled with indo-1-AM at 5 μg/ml for 20 min. at 37°C, as described (27).

Phagocytosis of erythrocytes

SRBCs (Alsevers; Rockland Scientific, Gilbertsville, PA) were opsonized with rabbit anti-sheep E Ab (ICN Pharmaceuticals, Costa Mesa, CA) as described (28). SRBCs were added to neutrophils adherent to quartz coverslips at E:T 20:1 for 30 min at 37°C. Nonadherent SRBCs were removed by gentle washing.

Microscopy

Cells were observed microscopically at 37°C. Cells were suspended in HBSS containing glucose but not phenol red. Experiments were performed with quartz or Swiss glass coverslips; some glass contains chromium inclusions, which absorb and emit light in the same region as indo-1. Each microscope slide was scanned to identify morphologically polarized cells with well-defined uropods.

Microfluorometry and excitation spectrophotometry

Quantitative microfluorometry and excitation spectroscopy were performed on single cells using a Peltier-cooled PMT D104 system (Photon Technology, Lawrenceville, NJ) attached to a Zeiss Axiovert 35 (Carl Zeiss, New York, NY) fluorescence microscope. A monochromator and a fiber-optically coupled xenon lamp were controlled by FeliX software (Photon Technology). During microfluorometry, the excitation and emission wavelengths were set using excitation at 350 nm (10 nm band-pass), and emission was detected using a 400LP dichroic mirror and a 405DF43 emission filter. The PMT output was plotted as a function of time. For excitation spectroscopy, a 400-nm long-pass dichroic mirror and either a 405DF43 emission filter or a 490DF20 emission filter were used. Excitation spectra were processed by FeliX software. The excitation spectra shown are an average of 10 spectra each accumulated with a 0.2-s integration time and a 1-nm step size.

High speed imaging and emission spectroscopy

High speed imaging was performed using an Axiovert 135 fluorescence microscope with a quartz condenser, quartz objective, and an AttoArc mercury lamp (Carl Zeiss). In the high wavelength region, a 365WB50 exciter, a 400LP dichroic mirror, and a 490DF20 emission filter were used. To image the low wavelength indo-1 region, a 365WB50 exciter, 400LP dichroic mirror and a 418LP emission filter or, for improved contrast, a 355HT15 exciter, a 390LP dichroic reflector, and a 405DF43 emission filter were used. To increase light collection efficiency, the bottom port of the microscope was used. This port was fiber-optically coupled to the input of an Acton-150 (Acton Instruments, Acton, MA) imaging spectrophotometer. The fiber optic coupling results in a substantial gain in light collection efficiency (29). In comparison with a similar Zeiss inverted scope using optical elements to relay the light to a PMT, the throughput of this modified microscope was improved greatly. The exit side was connected to a liquid N_2-cooled intensifier attached to a Peltier-cooled I-MAX-512 camera (approximately −20°C) (Princeton Instruments, Trenton, NJ) (27–29). A Gen-II tube was used to provide maximal efficiency in the violet-blue region of the spectrum (30). The camera was controlled by a high speed Princeton ST-133 interface and a Stanford Research Systems (Sunnyvale, CA) DG-535 delay gate generator (26). To improve computer acquisition times, the size of the pixel array was adjusted. A Dell Precision 410 workstation with an 800-MHz processor, 1.0-Gb RAM, 16-Mb onboard cache, and a high speed Lava Dual PCI enhanced port (Lava Computer, Toronto, Canada) was used. Winspec (Princeton Instruments) software was used. Winspec CPU calls were given system priority to enhance the instrument's duty cycle. Data were acquired without reporting to the monitor to further improve system speed. Data capture used a software-allocated RAM disk. For emission spectroscopy, the mirror in the Acton unit was replaced with a ruled grating (300 grooves/mm) (23). A schematic diagram of the apparatus is shown in Fig. 1.

As illustrated in Figs. 4–6, calcium spikes lasting for 200 ms occur once every 20 s. Because only a few seconds of high speed acquisition were possible (depending on the duty cycle of the instrument), it was necessary to note the arrival time of calcium spikes in the live spectrum-analysis mode of the Winspec software and then manually trigger high speed acquisition before the arrival of the calcium spike. Thus, in many cases "clipping" at the beginning or end of the movies occurred whereas in other cases the spike was missed altogether. The instability of the Windows operating environment also contributed to data loss. The number of independent experiments is listed below as n. The number of successful high speed movies is given as m.

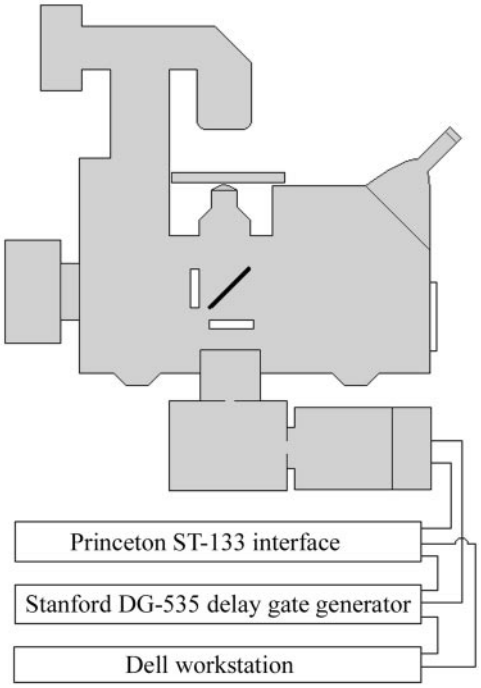

FIGURE 1. Schematic diagram of the apparatus for high speed imaging and spectroscopy. The diagram shows a Zeiss IM135 scope, as described in *Materials and Methods*, interfaced to the detection and data-handling electronics.

Results

Spectral characterization of system performance

The fluorescent calcium probe indo-1 was chosen because it can be used in nonratiometric experiments (31), a necessity at high data acquisition speeds. Fig. 2*a* shows four indo-1 emission spectra collected at different Ca^{2+} concentrations using microspectrophotometry. Emission intensity is a function of Ca^{2+} concentration and wavelength; the lower wavelength peak at 415 nm increases with Ca^{2+} concentration, whereas the higher wavelength peak decreases in intensity. According to Fig. 2*a*, cells imaged at 415 nm should brighten as Ca^{2+} levels increase, whereas cells imaged at 490 nm should darken. This is confirmed in Fig. 2, *b* and *c*, wherein the local Ca^{2+} signal becomes brighter in Fig. 2*b* at 415 nm but dimmer in a separate experiment (Fig. 2*c*) at 490 nm. We have also confirmed the presence of Ca^{2+} spikes in polarized neutrophils (15) using quantitative microfluorometry at ~415 nm (Fig. 2*d*) and 490 nm (Fig. 2*e*). In both experiments the interspike interval is ~20 s. This interval decreased to ~10 s. after exposure to neutrophil activating stimuli such as FMLP, as previously described (32, 33). Spikes were not observed for resting cells or unlabeled polarized cells (data not shown). These data show that the spike duration is 210 ms, although it does not provide spatial details. Because the dynamic range is greater near 415 nm, this spectral region was used in subsequent experiments.

Several additional experiments were performed to characterize the physical and chemical properties of indo-1 in neutrophils. Although Fig. 2*a* shows that the emission intensities differ when monitored at 415 and 490 nm, we sought to confirm the similarity in the excitation properties of indo-1 at these emission wavelengths in this system. We therefore performed excitation spectroscopy on adherent indo-1-labeled neutrophils. Fig. 3 shows representative excitation spectra of an indo-1-labeled neutrophil as

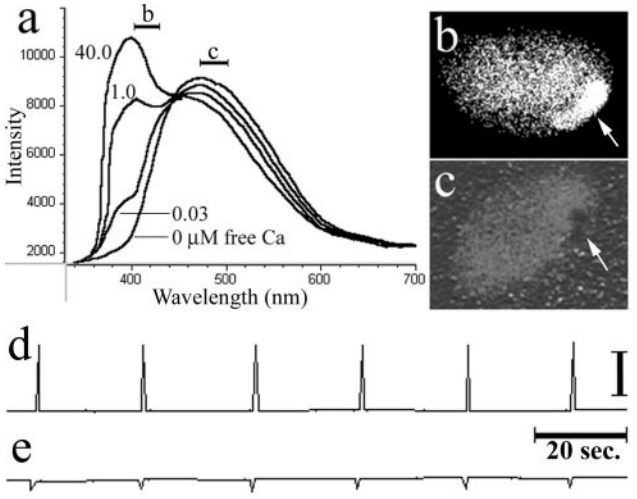

FIGURE 2. Emission spectroscopy, imaging, and microfluorometry of indo-1. *a*, Indo-1 and various Ca^{2+} concentrations were encased in a thin layer of gelatin and then studied by emission microspectrophotometry. The emission peaks are sensitive to Ca^{2+} concentration (28). Bars b and c approximate the spectral regions used in panels *b* and *c*. *b* and *c*, Ca^{2+} signaling was studied by high speed microscopy using a 100-ns shutter speed. In *b*, an emission filter in the region of 415 nm was used and showed a bright region high in Ca^{2+} rotating about the periphery of the cell (arrow). In *c*, an emission filter at 490 nm was used. At 490 nm, the emission intensity of indo-1 decreases at a higher calcium concentration, thus leading to a dark region high in Ca^{2+} rotating about the cell periphery (arrow). ×1260; $n = 4$, $m = 22$). *d* and *e*, Ca^{2+} spikes within polarized neutrophils. The spectral regions used in *d* and *e* were 415 and 490 nm, respectively. Bar, 2000 counts ($n = 4$).

measured at the emission wavelengths of 415 and 490 nm. As these spectra show, the wavelength dependence of indo-1 excitation is very similar for the two emission wavelengths. Thus, the excitation properties of indo-1 do not depend on the emission wavelength.

Detection of Ca^{2+} signals in polarized neutrophils

Inasmuch as fluorescent Ca^{2+} indicators may act as intracellular buffers, we next confirmed that the indo-1 labeling protocol did not lead to significant buffering of Ca^{2+} signals. To accomplish this goal, quantitative microfluorometry experiments were conducted on indo-1-labeled neutrophils, as described above, except that different concentrations of indo-1 were used in the labeling procedure. After labeling, the cells were washed extensively then resuspended in HBSS (without Ca^{2+}, Mg^{2+}, or phenol red). Fig. 4 shows quantitative microfluorometry of polarized neutrophils labeled with different concentrations of indo-1 for 20 min. Although the Ca^{2+} spike interval may vary slightly from cell to cell, the amplitude of the spike is clearly dependent on the concentration of indo-1 used in the labeling protocol. Importantly, at an indo-1 concentration of 35 μg/ml, the amplitude of the Ca^{2+} spikes decreases. This reduction in amplitude at 35 μg/ml is likely due to the ability of indo-1 to buffer Ca^{2+} signals. Thus, we find no evidence for indo-1-mediated buffering at the indo-1 concentration used in these studies (5 μg/ml). We next independently confirmed that indo-1 in neutrophils was responding to Ca^{2+}. Previous studies have shown that neutrophils are able to polarize during conditions of Ca^{2+} buffering (34). We therefore studied polarized neutrophils labeled with indo-1 in HBSS in the absence of external divalent cations. Cells were studied in a microscope chamber that allowed the addition of external solutions. The intracellular Ca^{2+} buffer BAPTA-AM was chosen because other molecules, such as 2-[(2-bis[carboxymethyl]amino-5-methylphenoxy)methyl]-6-methoxy-8-bis[carboxymethyl]aminoquinolone, would interfere with the fluorescence studies. BAPTA-AM was added to cells at a final concentration of 30 μM during observations at 37°C. As Fig. 5*a* shows, ~2 min after addition of BAPTA-AM to polarized neutrophils, the intensity of the Ca^{2+} spikes begin to diminish progressively. BAPTA-AM diffuses into the cell where it is cleaved to form BAPTA. We suggest that the reduction in indo-1 intensity is due to the buffering capacity of BAPTA; intracellular Ca^{2+} buffering capacity increases as BAPTA-AM enters the cell, thereby progressively decreasing spike amplitude. Furthermore, the constancy of the Ca^{2+} spike amplitudes in Figs. 2*d*, 4, and 5*b* (and data not shown) indicate that significant photobleaching is not occurring under the conditions used. Therefore, the gradual reduction

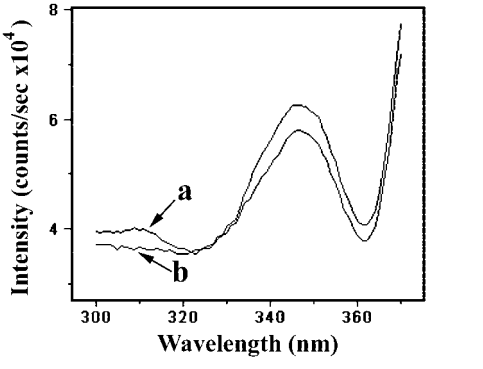

FIGURE 3. Excitation spectroscopy of indo-1. Indo-1-labeled neutrophils were examined by excitation microspectrophotometry. Excitation wavelengths were scanned using a xenon lamp and monochrometer. Emission intensities were detected at 490 nm (*trace a*) and 405 nm (*trace b*) using emission filters and a PMT assembly (Photon Technologies). Note the similarities in the excitation spectra ($n = 3$).

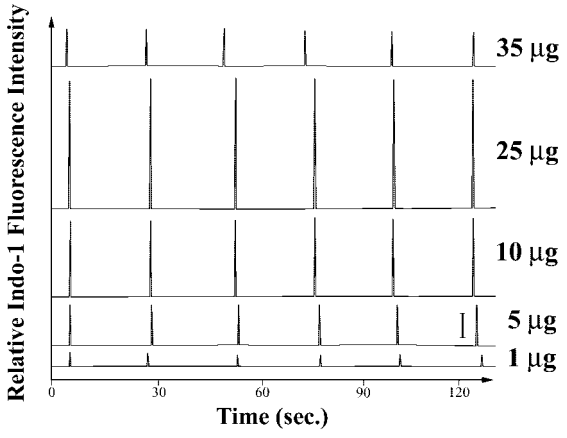

FIGURE 4. Representative examples of Ca^{2+} spikes within polarized neutrophils using different loading concentrations of indo-1-AM. Quantitative microfluorometry studies showing Ca^{2+} spikes within separate polarized neutrophils after loading with various extracellular concentrations of indo-1-AM from 1 to 35 μg/ml. The intensity of the Ca^{2+} spikes increases as the loading concentration of indo-1-AM is increased. However, the intensity decreases at 35 μg/ml, which is due to the buffering capacity of indo-1. For this reason, a concentration of 5 μg/ml, which gives a sufficient intensity but does not promote buffering, was generally used in these studies. To conserve space, data are plotted as relative (not absolute) intensity vs time. (The baseline fluorescence intensity was greatly increased in cells labeled at an indo-1-AM concentration of 35 μg/ml.) Bar, 2000 counts ($n = 3$).

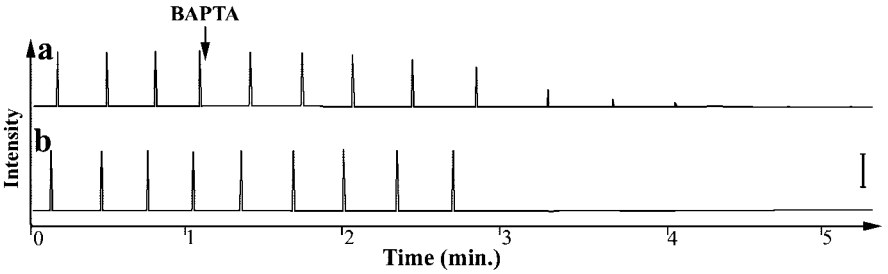

FIGURE 5. Effect of Ca^{2+}-sequestering agent BAPTA on Ca^{2+} spikes in neutrophils. Indo-1-labeled neutrophils were allowed to polarize on coverslips. Ca^{2+} spikes were followed over time using a PMT. When BAPTA-AM was added to the chamber to a final concentration of 30 μM, the fluorescence intensity of indo-1 gradually diminished (*a*), in contrast to the effect of BAPTA, when neutrophils become spherical the Ca^{2+} spikes abruptly end without gradual diminution (*b*). Bar, 2000 counts ($n = 3$).

in Ca^{2+} spike intensity in Fig. 5*a* cannot be explained by photobleaching. However, one might argue that the Ca^{2+} signaling simply stopped in a manner unrelated to intracellular Ca^{2+} buffering by BAPTA; e.g., the cell may have simply returned to a resting morphology. In our experience with leukocytes and tumor cells, Ca^{2+} spikes do not significantly diminish in intensity during our observations. Fig. 5*b* shows a representative example of an indo-1-labeled neutrophil as the cell polarity was relaxed. This illustrates the fact that Ca^{2+} spikes end abruptly. Thus, our experiments were performed at an indo-1 concentration that 1) was substantially below the level of indo-1-mediated buffering and 2) responded to Ca^{2+}.

Although data presented above suggest that photobleaching is not significant during these experimental conditions, we sought to rigorously exclude this possibility. We therefore performed experiments over extended periods of time to ascertain the level of photobleaching. Ca^{2+} spikes were studied in polarized neutrophils during continuous illumination with a mercury lamp. Fig. 6 shows a representative long duration experiment covering 10 min of observation. In this experiment, the Ca^{2+} spike intensity decreased by ~0.2%/min. Similar results were obtained in other experiments. Therefore, photobleaching is not a significant problem in these studies. This result is not surprising because previous workers have noted that photobleaching is not a significant problem for indo-1-labeled adherent cells for up to 30 min of observation (35).

Temporal characterization of Ca^{2+} signal detection

Indo-1-labeled neutrophils were observed while adherent to quartz coverslips. The cells were observed from the basal to apical surfaces, as illustrated in Fig. 7*A*. To test the effect of shutter speed on images, the CCD chip was electronically gated for various times. Polarized neutrophils display repetitive Ca^{2+} spikes (15, 33). Fig. 8 shows six experiments of indo-1-labeled polarized cells at increasingly shorter shutter speeds (2 s to 50 ns). At relatively long exposure periods, the cell may appear somewhat brighter at the center such as in the second frame of Fig. 8*a*. This is due to the randomization of the bright indo-1- Ca^{2+} complex while the electronic shutter is open. Because neutrophils and most other cells are thicker near the center, they might appear brighter at the center at slow shutter speeds when there is no Ca^{2+} spike occurring (e.g., a spike is present in Fig. 2*a*, *frame 3*, but not in *frame 2*). No clear spatiotemporal patterns emerge until a shutter speed of 200 μs is reached. The image is improved by the shorter exposure time which 1) reduces the distance Ca^{2+} waves can travel, 2) reduces the ability of indo-1:Ca^{2+} complexes to move away from regions of high Ca^{2+} concentration, and 3) reduces the contribution of background fluorescence within the cell by a factor of 10^4 (from 2 s to 200 μs). Thus, gating times of $\leq$200 μs can detect Ca^{2+} signaling routes in this particular experiment.

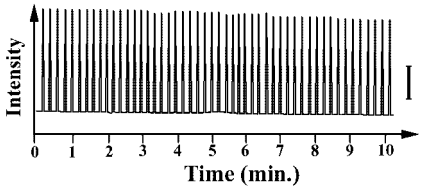

FIGURE 6. Effect of prolonged illumination on Ca^{2+} spike intensity. Indo-1-labeled neutrophils were allowed to polarize on coverslips. Ca^{2+} spikes were followed over extended periods of time using a PMT. A small loss in Ca^{2+} spike intensity was observed. In this representative example, a 3% reduction in spike intensity was found after 12 min. Thus, photobleaching of the fluorescent indo-1:Ca^{2+} complexes is not likely to seriously affect the spatial analyses of Ca^{2+} spikes shown below. Bar, 2000 counts ($n = 3$).

Calcium signaling routes in polarized neutrophils

Fig. 9 shows one cell with each Ca^{2+} spike divided into multiple frames using a 50-ns exposure time and a 20-ms delay time between frames. Ca^{2+} does not rise uniformly during a spike: it is highly asymmetrical and time dependent (Fig. 9*A*). The Ca^{2+} signal follows a pathway near the cell surface in a counterclockwise direction, as viewed from the basal to apical surfaces (Fig. 7*A*). The direction of Ca^{2+} wave travel, in this case counterclockwise, is not meant in an absolute sense, but rather in the laboratory frame of reference (Fig. 7*A*). Thus, the terms counterclockwise and clockwise are used only for illustrative purposes to differentiate between the types of high speed waves (Fig. 7*B*). The Ca^{2+} signal begins near the center of the lamellipodium and then travels unidirectionally in all cells observed (Fig. 9*A*). The calcium wave traveled with a velocity of 180 $\pm$ 16 μm/s. Furthermore, the Ca^{2+} wave terminated when it returned to the ignition site. Thus, for polarized neutrophils, the ignition site, termination site, and velocity did not vary significantly. Moreover, intracellular Ca^{2+} signals possess inherent asymmetries (i.e., directionality), like the unidirectional propagation of action potentials along an axon.

Because chemotactic agents cause Ca^{2+} release from internal stores and an influx of extracellular Ca^{2+} (36), we tested the ability of FMLP to affect Ca^{2+} patterns. A physiologically relevant dose of 50 nM FMLP triggered two Ca^{2+} waves traveling in opposite directions (clockwise and counterclockwise). In the experiment of Fig. 9*B*, an FMLP (50 nM)-charged micropipet was within several micrometers of the cell. FMLP was thereby delivered to a specific region of the plasma membrane, as confirmed using a fluorescent FMLP analog (data not shown). As shown in Fig. 9*A*, Ca^{2+} signaling begins near the center of the lamellipodium and then propagates around the perimeter of the cell in a counterclockwise direction. When this Ca^{2+} wave reaches the FMLP binding site, a second Ca^{2+} wave moving in a clockwise direction emanates from this point (Fig. 9*B*) which eventually becomes a new lamellipodium. The two waves propagate around the perimeter of the cytoplasm, cross at the opposite side of the cell and then continue until they return to the FMLP binding site. The counterclockwise and clockwise waves travel with the same velocity of ~180 μm/s.

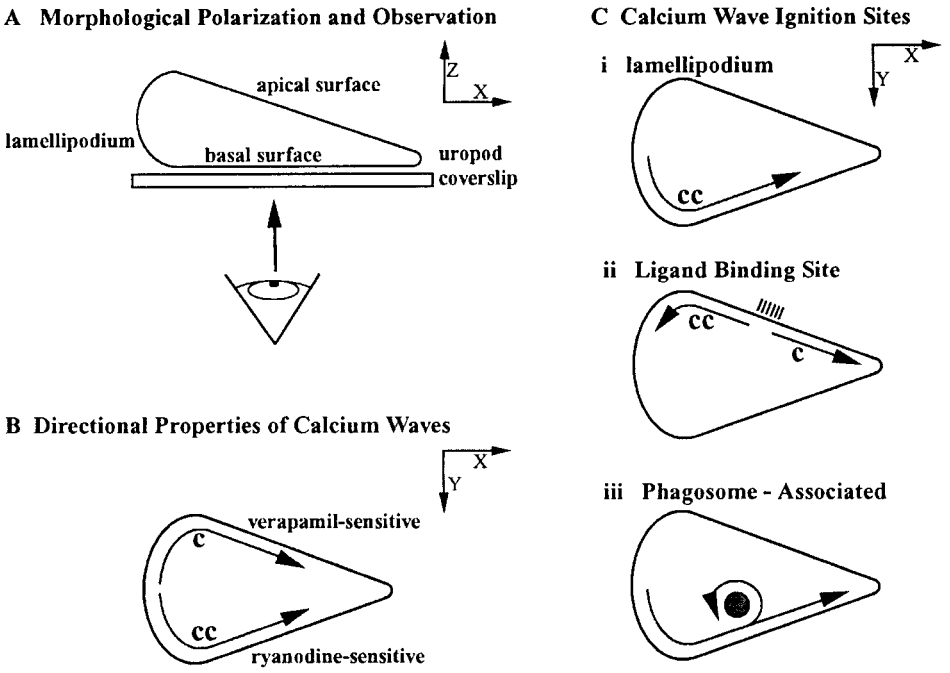

FIGURE 7. Summary of the observational geometry and wave directions observed. *A,* Cells were observed on an inverted fluorescence microscope at 37°C from the basal toward the apical surfaces. *B,* With this observational geometry, polarized neutrophils were found to exhibit Ca^{2+} waves traveling in either counterclockwise (cc) or clockwise (c) directions. *C,* Ca^{2+} waves originate from several cellular sites including the lamellipodium, ligand binding sites, and the plasma membrane near sites of phagocytosis.

These spatial and temporal findings are generally true, but the total distance traveled depends on the location of FMLP binding. For example, when FMLP is applied at the uropod (data not shown), the first wave does not travel as far before splitting into two waves. The next Ca^{2+} spike is a single Ca^{2+} wave that begins at the FMLP binding site and propagates in a counterclockwise direction (Fig. 9*C*). These events were restricted to productive engagement of the formyl peptide receptor because the antagonist Boc-Phe-Leu-Phe-Leu-Phe did not affect the Ca^{2+} signaling pattern (data not shown).

To characterize these signals, pharmacological probes were used. When neutrophils were exposed to saturating doses of ryanodine, which blocks endoplasmic reticulum (ER) Ca^{2+} release, the cells did not polarize normally. We therefore titered ryanodine to find that 10 μg/ml did not significantly affect cell shape. When the cells were observed with high speed imaging, a Ca^{2+} wave was initiated at the lamellipodium but disappeared during propagation (Fig. 10*A*). Thus, the counterclockwise Ca^{2+} release is ryanodine sensitive, suggesting the involvement of ryanodine receptors in wave propagation. In contrast, the plasma membrane channel blocker verapamil had no effect on the counterclockwise wave in polarized cells (data not shown). However, verapamil (100 μM) did block the clockwise-propagating wave in neutrophils exposed to FMLP during imaging experiments (Fig. 10*B*). This verapamil concentration is consistent with interference with K^+ channels. The clockwise wave was also blocked by chelation of extracellular Ca^{2+} using EDTA. In this experiment indo-1-labeled adherent cells were washed three times with Ca^{2+}-free PBS then suspended in PBS containing 1 mM EDTA. When polarized cells were stimulated with FMLP, only one counterclockwise Ca^{2+} wave was observed (Fig. 10*C*). Therefore, it seems likely that plasma membrane channels participate in propagation of the clockwise Ca^{2+} wave. In addition, the actions of these Ca^{2+} inhibitors reconfirm that these waves (or spikes) are due to Ca^{2+}. Because the clockwise wave is not initiated in the presence of ryanodine, the role of ryanodine receptors in this pattern element cannot be discerned. These waves correlate with cell polarity and receptor binding and represent a very early intracellular event in direction finding. Thus, extracellular spatial information is transduced into intracellular spatial information.

Calcium signaling routes surround phagocytic targets

We next tested the potential breadth of Ca^{2+} signaling waves during a distinct physiological process. Phagocytosis has been associated with Ca^{2+} spikes (15). Indo-1-labeled neutrophils were incubated with IgG-opsonized SRBCs on the 37°C stage of the

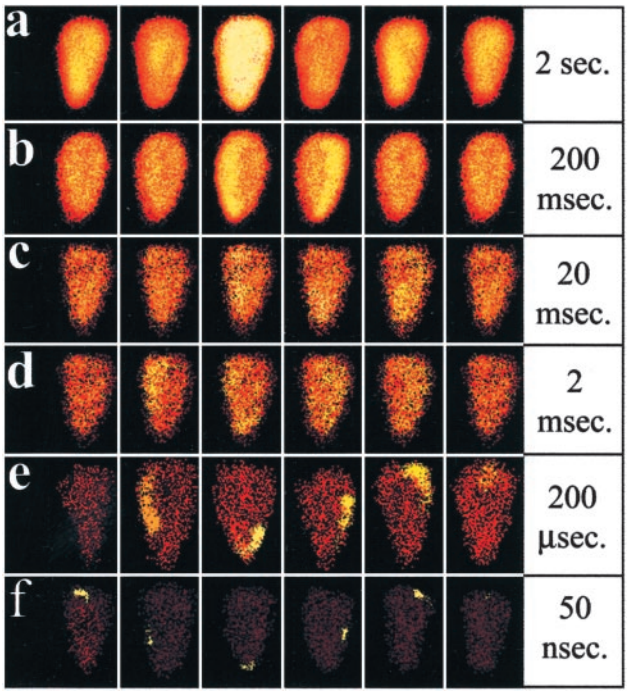

FIGURE 8. Effect of exposure time on the appearance of indo-1 labeled polarized neutrophils. Images with exposure times of 2 s to 50 ns were obtained with a 30-ms duty cycle. Clear spatiotemporal Ca^{2+} patterns can be recognized at 200 μs and below ($n = 3$). ×960.

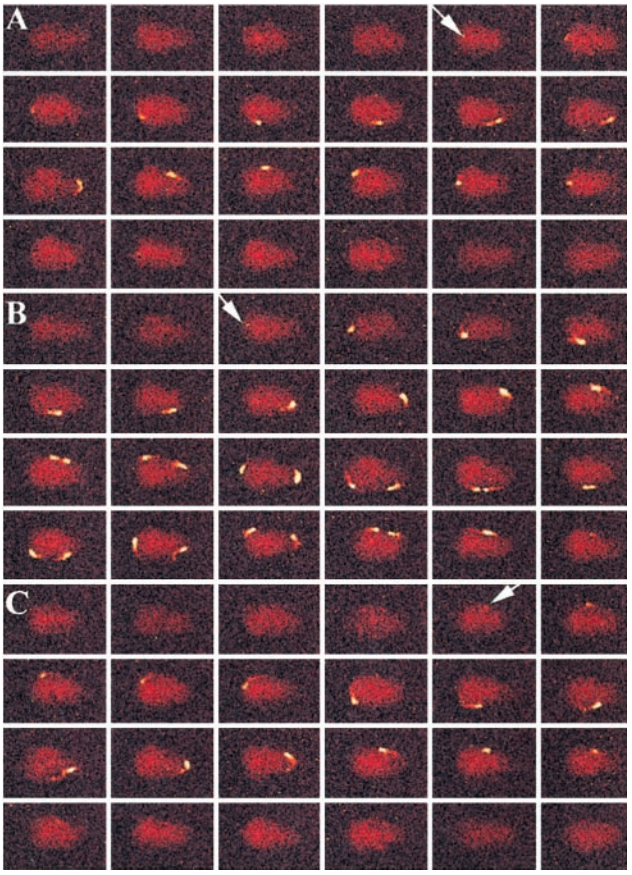

FIGURE 9. High speed imaging reveals that Ca^{2+} spikes are Ca^{2+} waves propagating in the perimembrane region of polarized neutrophils. *A,* Micrographs of indo-1-labeled cells were acquired using a 100-ns shutter speed and a 30-ms duty cycle. *A–C,* Micrograph sequences shown in represent consecutive spikes observed for a single polarized neutrophil. A Ca^{2+} wave begins at the lamellipodium and propagates in a counterclockwise direction. *B,* At a time between the sequence shown in *A* and *B,* a micropipet charged with 50 nM FMLP was discharged within a few micrometers of the cell surface to stimulate formyl peptide receptor on one side of the cell (at the top of the micrograph). In this sequence, the Ca^{2+} signal begins at the old lamellipodium and then propagates about the periphery of the cell until it reaches the FMLP binding site. At this point, the counterclockwise wave becomes two Ca^{2+} waves traveling in opposite directions. Both Ca^{2+} waves continue propagating around the cell until they return to the FMLP binding site. *C,* The next Ca^{2+} spike begins at the site of FMLP binding (arrow) and then propagates about the periphery of the cell as a single unidirectional wave. Thus, environmental directional cues are transduced into oriented spatial patterns ($n = 4$, $m = 34$). ×840.

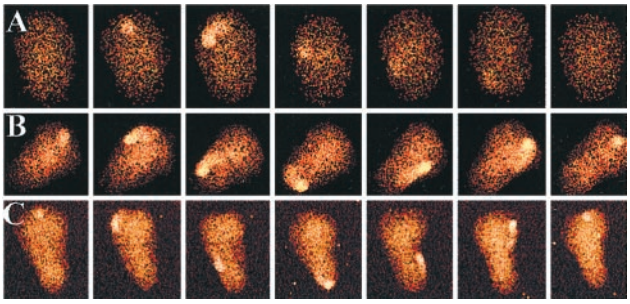

FIGURE 10. Pharmacological agents suggest that clockwise and counterclockwise Ca^{2+} waves originate from extracellular and intracellular sources. *A,* Suboptimal doses of ryanodine interfere with the propagation of counterclockwise waves. *B,* Verapamil blocks the appearance of clockwise waves during FMLP addition. *C,* The appearance of the clockwise waves was also blocked in a Ca^{2+}-free buffer containing EDTA ($n = 5$, $m = 28$). ×920.

microscope. Ca^{2+} signaling was imaged at high speed (50 ns exposure time and 20 ms delay time). As Fig. 11 shows, the Ca^{2+} signal begins at the lamellipodium and then propagates in a counterclockwise direction about the periphery of the cell. As this first Ca^{2+} wave passes the target, another Ca^{2+} wave appears to split off from the first, followed by its propagation in a counterclockwise manner about the perimeter of the target. As the differential interference contrast image illustrates (Fig. 11, *frame 1*), the dark circular regions in the fluorescence micrographs correspond to the two IgG-opsonized targets. By adjusting the focus of the microscope, the targets were found to be internalized, although the phagosome nearer the lamellipodium appeared to have completed phagocytosis just before Ca^{2+} imaging was initiated. In this example, the Ca^{2+} wave appears to travel intracellularly from one phagosome to a neighboring phagosome (Fig. 11, *frame 15*). In other examples of multiple target uptake where the targets are separated by several micrometers (data not shown), the Ca^{2+} wave travels from the region of the cell surface to the phagosomes. Thus, there appear to be at least two routes of Ca^{2+} signaling in the vicinity of phagosomes. When cells were treated with ryanodine as described above, Ca^{2+} wave propagation about the phagosomes was not observed (data not shown). This is consistent with the reported intracellular origin of Ca^{2+} signals mediating phagolysosome formation. Because phagocytosis takes place at very low Ca^{2+} levels (37), we suggest that these Ca^{2+} waves promote the formation of phagolysosomes, which does require Ca^{2+} signaling (38, 39). Although these Ca^{2+} waves resemble those associated with chemotactic stimulation, they differ in their location. Thus, a diversity of Ca^{2+} signaling routes can be observed during physiological events.

Discussion

Intracellular Ca^{2+} plays a pivotal role in many cell functions. It has been linked with neutrophil functions such as production of reactive oxygen species, chemotaxis, phagolysosome formation, degranulation, adherence, and integrin recycling (9, 10, 15, 34, 40–45). At the cellular level, Ca^{2+} changes are often seen as temporally short and intense bursts, also known as spikes. Ca^{2+} spikes occur during neutrophil adherence, phagocytosis, and migration (15, 41). However, the spatiotemporal dynamics of Ca^{2+} signaling in neutrophils and many other cell types are essentially unknown. To map dynamic signaling events, we have used modern electro-optic technology and an efficient optical microscope (23–25) that allows both high repetition rates and short exposure times. When indo-1-labeled cells are imaged for a relatively long period of time, the indo-1:Ca^{2+} emission resembles that obtained using conventional video microscopy. However, when the CCD chip is gated for short periods of time, punctate indo-1:Ca^{2+} emission is observed traveling near the plasma membrane. A theoretical study by Simon and Llinas (46) predicted intense submembrane Ca^{2+} profiles at submicrosecond time scales. Our experimental findings are consistent with these calculations. Moreover, the repetition rates available with our apparatus make it is possible to follow the trafficking of Ca^{2+} signals from place to place within a living cell.

High speed microscopy has revealed that Ca^{2+} is not homogeneously distributed within a polarized cell during a spike; instead, Ca^{2+} waves follow apparently specific and highly reproducible signaling routes. In other words, the Ca^{2+} spike of a neutrophil is a rapidly traveling Ca^{2+} wave when resolved spatiotemporally. These findings provide exciting new insights in cell signaling. For

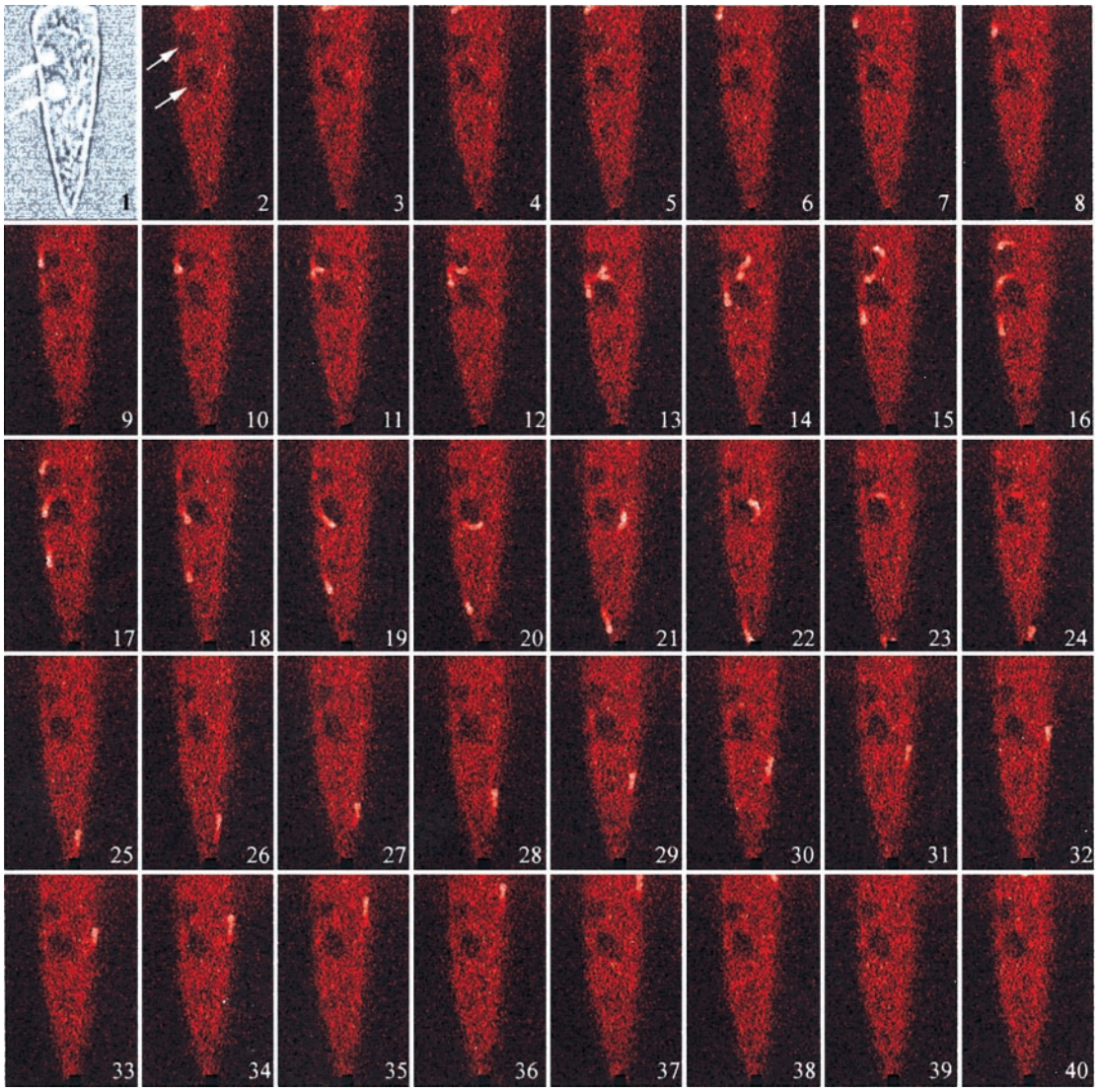

FIGURE 11. Phagosomes exhibit counterclockwise traveling Ca^{2+} waves. High speed fluorescence microscopy of indo-1-labeled neutrophils was performed using the 355HT15/390LP/405DF43 filter set. Cells were allowed to bind and phagocytose IgG-opsonized SRBCs. The erythrocytes were not labeled with indo-1 and therefore appear dark in the micrographs. A polarized neutrophil with associated erythrocytes are shown in the differential interference contrast image of *frame 1*. In addition to the counterclockwise wave traveling near the cell surface (Fig. 3, *trace a*), an additional counterclockwise wave appears to split off the perimembrane wave (*frames 12* and *13*) and travel about the upper target (*frames 13–20*). A third Ca^{2+} wave appears to split off from the first target (*frame 15*) and then travel about the perimeter of second target (*frames 15–25*), while the original Ca^{2+} wave (*frames 2–40*) continues its journey about the cell periphery ($n = 3$, $m = 15$). ×1340.

example, we speculate that the Ca^{2+} signaling routes defined above reflect the subcellular control mechanisms participating in cell orientation and phagolysosome formation. Morphologically polarized cells exhibit one ryanodine-sensitive Ca^{2+} wave propagating in a counterclockwise direction around a cell. During chemotactic stimulation, two Ca^{2+} waves traveling in clockwise and counterclockwise directions, likely associated with both external and internal Ca^{2+} stores, are observed. The clockwise Ca^{2+} wave does not occur immediately after binding; ligated receptors must wait until the counterclockwise-rotating wave reaches the FMLP binding site. When the single wave reaches this site, Ca^{2+} signals are propagated in both directions. The counterclockwise wave and local receptor activation may act synergistically to reach a signaling threshold that allows ignition of a clockwise wave. This wait state, or phase delay, was anticipated by our temporal studies of neutrophil activation (47). These two Ca^{2+} waves orient in the direction of an extracellular ligand, like an intracellular compass.

Multiple Ca^{2+} waves are also seen after phagocytosis of IgG-opsonized SRBCs. However, in this case, the waves were found well within the cytoplasm of the neutrophil where they traveled in a counterclockwise direction around the target. We speculate that Ca^{2+} waves traveling about the perimeter of the phagosome participate in phagolysosome formation. However, these phagosome-associated Ca^{2+} waves differ from prevailing models of phagolysosome formation in that they were observed only in the presence of a pre-existing Ca^{2+} wave traveling near the plasma membrane or a neighboring phagosome. Thus, in addition to the physiological information encoded within the frequencies and amplitudes of Ca^{2+} spikes (2–8), high speed microscopy has revealed a Ca^{2+} spike may contain multiple types of spatiotemporal patterns, which we believe are also rich in information.

Our studies have shown that a direct line of communication exists between the Ca^{2+} signaling apparatus of the plasma membrane and that of the phagosome. Thus, the phagosome remains in

communication with the plasma membrane despite having pinched off from the plasma membrane. Several recent studies have suggested a role for the ER in phagocytosis. 1) The microorganisms *Legionella* and *Brucella* can reside within an ER-like region of phagosomes (48). 2) A proteomic analysis has identified the presence of ER components within phagosomes (49). 3) Mutants deficient in the ER proteins calreticulin and calnexin are deficient in phagocytosis. Moreover, green-fluorescent protein-labeled calreticulin and calnexin demonstrated a link between the ER and phagocytic cup (50). Thus, we suggest that a strand of the ER mediates the line of communication indicated by the present study. Although we have not studied the mechanism of Ca^{2+} signal migration from cell surfaces to intracellular membranes, a direct coupling between the L-type Ca^{2+} channels of the plasma membrane and ryanodine receptors on internal ER membranes is a possibility (51, 52), given that we have preliminary evidence suggesting the presence of L-type channels on neutrophils (our unpublished observations). The characteristics of the assembly and regulation of this signaling conduit in living cells will likely contribute to a molecular understanding of why certain receptors do not promote phagolysosome fusion and certain microorganisms escape phagolysosomal destruction.

In addition to its location, a wave is also described by a velocity. The velocity of the perimembrane Ca^{2+} wave is 180 μm/s. Although this velocity has been observed in all of the experiments described here, a spherically expanding Ca^{2+} wave with a velocity of $\sim$30 μm/s has been observed during neutrophil adherence (our unpublished observations), which presumably represents a distinct propagation mechanism. The velocity of $\sim$180 μm/s is substantially slower than the velocity of membrane depolarization seen in unmyelinated axons, yet faster than that seen for other Ca^{2+} waves (16–19) or expected based on the measured diffusion coefficient of Ca^{2+} (53). A mechanism involving both membrane potential and short range diffusion might account for these observations. One likely participant is inositol 1,4,5-triphosphate, which is generated during FMLP stimulation of neutrophils (54). Inositol 1,4,5-triphosphate promotes Ca^{2+} release from the ER, which in turn triggers store-operated Ca^{2+} influx across the plasma membrane (55). Recently, phosphoinositol 3-kinase-γ knockout mice have been shown to be defective in orientation in the presence of a chemotactic factor (56); this defect may be associated with the second clockwise Ca^{2+} wave.

The literature reports a Ca^{2+} concentration of $\sim$400 nM during neutrophil activation (27). This concentration is spatially and temporally averaged over an entire cell or a population of cells. However, our data show that the Ca^{2+} concentration is not temporally or spatially uniform. The Ca^{2+} concentration near a plasma membrane may be far greater than the average concentration. For example, a concentration of 25 μM Ca^{2+} is required to mediate neutrophil degranulation in permeabilized cells (57), yet concentrations of only 400 nM are observed in stimulated neutrophils. Inspection of Figs. 8 and 10 show that local Ca^{2+} levels near plasma membranes and phagosomes are far higher than its bulk concentration, thus potentially accounting for the apparent discrepancy. Moreover, enzymes and cytoskeletal structures presumed to be insensitive to Ca^{2+} due to micromolar K_d may actually be sensitive when the spatiotemporal dynamics of the signal are considered.

The high speed microscopic imaging techniques outlined in this and previous papers (23–26) were designed to permit analyses of chemical wave propagation events within immune cells and should be generally applicable. For example, interactions been leukocytes and targets such as microbes and tumor cells is one potential area of interest. Preliminary studies in this laboratory suggest Ca^{2+} signaling coherence between neutrophils and endothelial cells during their interactions. We speculate that intracellular signaling may be understood in terms of spatiotemporal variables. Because enzymes can respond to Ca^{2+}, ATP, NADPH, pH, cAMP, and other intracellular conditions and because Ca^{2+}, NAD(P)H, and pH exhibit various signaling patterns (23–26), a variety of superimposed spatiotemporal patterns could be generated. Hence, a few chemicals, each with a set of characteristic patterns, could generate many spatiotemporal enzyme activity patterns. Using gene knockout mice, it should also be possible to identify proteins participating in various pattern elements. Lastly, we speculate that differences in emergent chemical patterns may explain certain difficulties encountered during rational drug development.

References

1. Petty, H. R. 1993. *Molecular Biology of Membranes*. Plenum Press, New York.
2. Dolmetsch, R. E., R. S. Lewis, C. C. Goodnow, and J. I. Healy. 1997. Differential activation of transcription factors induced by Ca^{2+} response amplitude and duration. *Nature 386:855.*
3. Berridge, M. J. 1997. The AM and FM of calcium signaling. *Nature 386:759.*
4. Gu, X., and N. C. Spitzer. 1995. Distinct aspects of neuronal differentiation encoded by frequency of spontaneous Ca^{2+} transients. *Nature 375:784.*
5. Putney, J. W. 1998. Calcium signaling: up, down, up, down. . . what's the point? *Science 279:191.*
6. De Koninck, P., and H. Schulman. 1998. Sensitivity of CaM kinase II to the frequency of Ca^{2+} oscillations. *Science 279:227.*
7. Goldbeter, A. 1996. *Biochemical Oscillations and Cellular Rhythms.* Cambridge University Press, Cambridge.
8. Tsien, R. W., and R. Y. Tsien. 1990. Calcium channels, stores, and oscillations. *Annu. Rev. Cell Biol. 6:715.*
9. Sawyer, D. W., J. A. Sullivan, and G. L. Mandell. 1985. Intracellular free calcium localization in neutrophils during phagocytosis. *Science 223:663.*
10. Brundage, R. A., K. E. Fogarty, R. A. Tuft, and F. S. Fay. 1993. Chemotaxis of newt eosinophils: calcium regulation of chemotactic response. *Am. J. Physiol. 34:1527.*
11. Thorn, P., A. M. Lawrie, P. M. Smith, D. V. Gallacher, and O. H. Peterson. 1993. Local and global cytosolic Ca^{2+} oscillations in exocrine cells evoked by agonists and inositol trisphosphate. *Cell 74:661.*
12. Kasai, H., Y. X. Li, and Y. Miyashita. 1993. Subcellular distribution of Ca^{2+} release channels underlying Ca^{2+} waves and oscillations in exocrine pancreas. *Cell 74:669.*
13. Thomas, A. P., D. C. Renard, and T. A. Rooney. 1991. Spatial and temporal organization of calcium signalling in hepatocytes. *Cell Calcium 12:111.*
14. Jacob, R. 1990. Imaging cytoplasmic free calcium in histamine stimulated endothelial cells and in fMet-Leu-Phe stimulated neutrophils. *Cell Calcium 11:241.*
15. Marks, P. W., and F. R. Maxfield. 1990. Transient increases in cytosolic free calcium appear to be required for the migration of adherent human neutrophils. *J. Cell Biol. 110:43.*
16. Lechleiter, J. D., and D. E. Clapham. 1992. Molecular mechanisms of intracellular calcium excitability in *X. laevis* oocytes. *Cell 69:283.*
17. Wussling, M. H., and H. Salz. 1996. Nonlinear propagation of spherical calcium waves in rat cardiac myocytes. *Biophys. J. 70:1144.*
18. Newman, E., and K. R. Zahs. 1997. Calcium waves in retinal glial cells. *Science 275:844.*
19. Takashima, I., M. Ichikawa, and T. Iijima. 1999. High-speed CCD imaging system for monitoring neural activity in vivo and in vitro, using a voltage-sensitive dye. *J. Neurosci. Methods 91:147.*
20. Zoghbi, M. E., P. Bolanos, C. Villalba-Galea, A. Marcano, E. Hernandez, M. Fill, and A. L. Escobar. 2000. Spatial Ca^{2+} distribution in contracting skeletal and cardiac muscle cells. *Biophys. J. 78:164.*
21. Takemura, H., S. Yamashina, and A. Segawa. 1999. Millisecond analyses of Ca^{2+} initiation sites evoked by muscarinic receptor stimulation in exocrine acinar cells. *Biochem. Biophys. Res. Commun. 259:656.*
22. Paemeleire, K., P. E. Martin, S. L. Coleman, K. E. Fogarty, W. A. Carrington, L. Leybaert, R. A. Tuft, W. H. Evans, and M. J. Sanderson, 2000. Intercellular calcium waves in HeLa cells expressing GFP-labeled connexin 43, 32, or 26. *Mol. Biol. Cell 11:1815.*
23. Petty, H. R., R. G. Worth, and A. L. Kindzelskii. 2000. Imaging sustained dissipative patterns in the metabolism of individual living cells. *Phys. Rev. Lett. 84:2754.*
24. Petty, H. R., and A. L. Kindzelskii. 2000. High-speed imaging of sustained metabolic target patterns in living neutrophils during adherence. *J. Phys. Chem. B 104:10952.*
25. Petty, H. R., and A. L. Kindzelskii. 2001. Dissipative metabolic patterns respond during neutrophil transmembrane signaling. *Proc. Natl. Acad. Sci. USA 98:3145.*
26. Kindzelskii, A. L., and H. R. Petty. 2002. Apparent role of traveling metabolic waves in periodic oxidant release by living cells. *Proc. Natl. Acad. Sci. USA 99:9207.*
27. Sehgal, G., K. Zhang, R. F. Todd, L. A. Boxer, and H. R. Petty. 1993. Lectin-like inhibition of immune complex receptor-mediated stimulation of neutrophils: effects on cytosolic calcium release and superoxide production. *J. Immunol. 150: 4571.*

28. Worth, R. G., L. Mayo-Bond, J. G. J. van de Winkel, R. F. Todd III, H. R. Petty, and A. D. Schreiber. 2001. The cytoplasmic domain of FcγRIIA (CD32) participates in phagolysosome formation. *Blood 98:3429.*
29. Roper Scientific Technical Note No. 6. www.roperscientific.com.
30. Roper Scientific Technical Note No. 11. www.roperscientific.com.
31. Haugland, R. P. 1996. *Handbook of Fluorescent Probes and Research Chemicals.* Molecular Probes, Eugene.
32. Kindzelskii, A. L., M. M. Eszes, R. F. Todd III, and H. R. Petty. 1997. Proximity oscillations of complement type 4 (α_X, β_2) and urokinase receptors on migrating neutrophils. *Biophys. J. 73:1777.*
33. Petty, H. R. 2001. Neutrophil oscillations: temporal and spatiotemporal aspects of cell behavior. *Immunol. Res. 23:125.*
34. Pierini, L. M., M. A. Lauson, R. J. Eddy, B. Henedey, and F. R. Maxfield. 2000. Oriented endocytic recycling of $\alpha_5\beta1$ in motile neutrophils. *Blood 95:2471.*
35. Wahl, M., M. J. Lucherini, and E. Gruenstein. 1990. Intracellular Ca^{2+} measurement with Indo-1 in substrate-attached cells: advantages and special considerations. *Cell Calcium 11:487.*
36. Merritt, J. E., R. Jacob, and T. J. Hallam. 1989. Use of manganese to discriminate between calcium influx and mobilization from internal stores in stimulated human neutrophils. *J. Biol. Chem. 264:1522.*
37. Di Virgilio, F., B. C. Meyer, S. Greenberg, and S. C. Silverstein. 1988. Fc receptor-mediated phagocytosis occurs in macrophages at exceedingly low cytosolic Ca^{2+} levels. *J. Cell Biol. 106:657.*
38. Majeed M., N. Perskvist, J. D. Ernst, K. Orselius, and O. Stendahl. 1998. Roles of calcium and annexins in phagocytosis and elimination of an attenuated strain of *Mycobacterium tuberculosis* in human neutrophils. *Microb. Pathog. 24:309.*
39. Jaconi, M. E., P. D. Lew, J. L. Carpentier, K. E. Magnusson, M. Sjögren, and O. Stendahl. 1990. Cytosolic free calcium elevation mediates the phagosome-lysosome fusion during phagocytosis in human neutrophils. *J. Cell Biol. 110: 1555.*
40. Hallett, M. B., E. V. Davies, and A. K. Campbell. 1990. Oxidase activation in individual neutrophils is dependent on the onset and magnitude of the Ca^{2+} signal. *Cell Calcium 11:655.*
41. Maxfield, F. R., and B. A. Kruskal. 1987. Cytosolic free calcium increases before and oscillates during frustrated phagocytosis in macrophages. *J. Cell Biol. 105: 2685.*
42. Jaconi, M. E., J. M. Theler, W. Schlegel, R. D. Appel, S. D. Wright, and P. D. Lew. 1991. Multiple elevations of cytosolic-free Ca^{2+} in human neutrophils: initiation by adherence receptors of the integrin family. *J. Cell Biol. 112: 1249.*
43. Lew, P. D., C. B. Wollheim, F. A. Waldvogel, and T. Pozzan. 1984. Modulation of cytosolic-free calcium transients by changes in intracellular calcium-buffering capacity: correlation with exocytosis and O_2-production in human neutrophils. *J. Cell Biol. 99:1221.*
44. Lawson, M. A., and F. R. Maxfield. 1995. Ca^{2+}- and calcineurin-dependent recycling of an integrin to the front of migrating neutrophils. *Nature 377:75.*
45. Demaurex, N., A. Monod, D. P. Lew, and K. Krause. 1994. Characterization of receptor-mediated and store-regulated Ca^{2+} influx in human neutrophils. *Biochem. J. 297:595.*
46. Simon, S. M., and R. R. Llinas. 1985. Compartmentalization of the submembrane calcium activity during calcium influx and its significance in transmitter release. *Biophys. J. 48:485.*
47. Albrecht, E., and H. R. Petty. 1998. Cellular memory: neutrophil orientation reverses during temporally decreasing chemoattractant concentrations. *Proc. Natl. Acad. Sci. USA 95:5039.*
48. Mesresse, S., O. Steele-Mortimer, E. Moreno, M. Desjardins, B. B. Finlay, and J. P. Gorvel. 1999. Controlling the maturation of pathogen-containing vacuoles: a matter of life and death. *Nat. Cell Biol. 1:E183.*
49. Garin, J., R. Diez, S. Kieffer, J.-F. Dermine, S. Duclos, E. Gagnon, R. Dadoul, R. Rondeau, and M. Desjardins. 2001. The phagosome proteome: insight into phagosome functions. *J. Cell Biol. 152:165.*
50. Muller-Taubenberger, A., A. N. Lupas, H. Li, M. Ecke, E. Simmeth, and G. Gerisch. 2001. Calreticulin and calnexin in the endoplasmic reticulum are important for phagocytosis. *EMBO J. 20:6772.*
51. Lu, X., L. Xu, and G. Meissner. 1994. Activation of the skeletal muscle calcium release channel by a cytoplasmic loop of the dihydropyridine receptor. *J. Biol. Chem. 269:6511.*
52. Marty, I., M. Robert, M. Villaz, K. De Jonh, Y. Lai, W. A. Catterall, and M. Ronjat, M. 1994. Biochemical evidence for a complex involving dihydropyridine receptor and ryanodine receptor in triad junctions of skeletal muscle. *Proc. Natl. Acad. Sci. USA 91:2270.*
53. Nasi, E., and D. Tillotson. 1985. The rate of diffusion of Ca^{2+} and Ba^{2+} in a nerve cell body. *Biophys. J. 47:735.*
54. Synderman, R., C. D. Smith, and M. W. Verghese. 1986. Model for leukocyte regulation by chemoattractant receptors: roles of a guanine nucleotide regulatory protien and polyphosphoinositide metabolism. *J. Leukocyte Biol. 40:785.*
55. Itagaki, K., K. B. Kannan, D. H. Livingston, E. A. Deitch, Z. Fekete, and C. J. Hauser. 2002. Store-operated calcium entry in human neutrophils reflects multiple contributions from independently regulated pathways. *J. Immunol. 168: 4063.*
56. Hannigan, M., L. Zhan, Z. Li, Y. Ai, D. Wu, and C.-K. Huang. 2002. Neutrophils lacking phosphoinositide 3-kinase γ show loss of directionality during *N*-formyl-Met-Leu-Phe-induced chemotaxis. *Proc. Natl. Acad. Sci. USA 99:3603.*
57. Smolen, J. E., S. J. Stoehr, and L. A. Boxer. 1986. Human neutrophils permeabilized with digitonin respond with lysosomal enzyme release when exposed to micromolar levels of free calcium. *Biochim. Biophys. Acta 886:1.*